Regularized Estimation for GNSS Positioning in Multipath/Non-Line-Of-Sight Environments

Nabil Kbayer, Mohamed Sahmoudi
TéSA Lab / ISAE, Toulouse University, FRANCE
E-mail: nabil.kbayer@isae.fr

***Abstract*— Considered as the free accessible and suitable solution for positioning in urban areas, Global Navigation Satellite Systems (GNSS) have been widely used these recent years in a wide spectrum of applications. However, signal blockage, non-line-of-sight (NLOS) multipath interferences and signal degradation affect the system performance and represent the major hurdles of GNSS in it course of adoption as a main localization technology in urban environments. Many approaches have been employed to constructively use these degraded signals in order to reduce positioning errors. Following this vision, we propose in this paper a joint estimation method of the position and the bias for measurement correction. This formulation leads to an ill-conditioned estimation problem. In this work, we apply a regularized robust estimation framework to this problem of NLOS mitigation for GNSS positioning in harsh areas. We derive the optimal regularization matrix by minimizing the total Mean Square Errors (MSE) of the considered model. The performance of the proposed method is assessed using real GNSS data collected in a dense urban area in Toulouse City, showing improvements in comparison to some existing methods.**

Keywords—GNSS; Multipath and NLOS reception; Positioning in urban environment; Regularized Estimation; Accuracy optimisation.

I. INTRODUCTION

Global Navigation Satellite Systems (GNSSs) are considered as the preferred solution for location and timing in a very wide and growing range of applications in urban areas. Nowadays, GNSS encompass many operational systems such as the American GPS, the Russian GLONASS and the European GALILEO, which forecast on a large increase of performance and services. However, even with this increase in the satellite availability and the improvement of the constellation geometry, GNSS positioning in urban areas suffer from degraded performance because of several problems that persist. On the other side, along with the appearance and innovation of new land applications, many of the demands come from urban environments where the processing needs of the received signals are extensively more complex than in open sky environments.

Harsh environments present significant challenges for satellite positioning that cater continuous accuracy and availability throughout the operation. Actually, the densely-built areas block direct GNSS signals, hence reduce the satellite visibility and increase the Dilution Of Precision (DOP) of remaining received signals. This presence of line-of-sight (LOS) blockage deteriorates the positioning accuracy for three reasons. First, it engenders very challenging technical issues for acquiring and tracking the attenuated GNSS signals. Hence, the continuity of position estimation cannot be guaranteed if tunnels, tall building and foliage disrupt the GNSS navigation completely. Secondly, urban environment, on the whole, consists of narrow streets and high buildings with smooth surfaces that may reflect the transmitted signals. Thus, it is very common that GNSS signals reach the receiver via multiple, direct and/or indirect, paths. Similarly, the satellite signal gets bent at the building edges and reaches the receiver where LOS is blocked by diffraction. Signals received in indirect paths can be classified into two separate types: Multipath (MP) signal if the signal is received through both direct and alternative paths and Non-Line-Of-Sight (NLOS) signal if the signal is received only through reflections. Besides, if the line of sight (LOS) is blocked and the satellite signal is received through a reflected NLOS path, the related pseudo-range (PR) measurement will be affected by an additional, positive and potentially unlimited in range [1]. These combined NLOS and multipath (MP) biases degrade the position estimation. Thirdly, the masking of the satellite signals induces a poor constellation geometry that may affect the Dilution Of Precision (DOP) unfavorably and hence degrade the positioning accuracy. In view of such technical challenges in urban areas, there is a pressing need to counteract the disadvantages of GNSS signal degradation and achieve user requirements in these harsh environments.

This paper is divided into five main sections. The first one presents the problem of GNSS positioning in urban environments. The second section proposes a brief review of the state on the MP/NLOS problem. In the third section, we illustrate the general GNSS problem statement and introduce our contributions on positioning in NLOS conditions. The fourth section outlines experimental results obtained in an urban canyon using GPS/GLONASS signals recorded in Toulouse (South-West of France). Finally, some conclusions are summarized in section 5.

II. MULTIPATH MITIGATION IN GNSS: STATE OF THE ART

Since the early years of GNSS, the problem of multipath mitigation has been extensively tackled in literature. Broadly speaking, the literature on the NLOS problem fall in three main categories: NLOS identification, NLOS mitigation and NLOS constructive use. The former tends to distinguish between "clean" LOS signals and NLOS range measurements.

Hardware-based distinction techniques include the use of a dual polarization antenna, a GNSS antenna array and a sky-pointing camera. Without using additional hardware, [1] proposes other indicators of NLOS reception such as elevation angle selection, C/N0-based NLOS detection and inter-satellite consistency checking [1]. Once NLOS measurements are identified, they can be either discarded [2], down-weighted [3] or used constructively to improve positioning [4-6].

The second approach typically tends to reduce the adverse impact of "deteriorated" NLOS signals on the estimation accuracy. Different configurations of antenna arrays are among the hardware solution for NLOS mitigation. Working in the receiver correlator output is another well-known approach. Several classical techniques for MP/NLOS mitigation exists in the literature and represents standard features of professional grade GNSS receivers, in particularly those based on narrow and double-delta correlators [7]. In-receiver MP mitigation methods include strobe correlator, the Multipath Estimating Delay Lock Loop (MEDLL) and Fast Iterative Maximum-Likelihood Algorithm (FILMA) [8]. However, characterized by their high complexity, these in-receiver techniques do not bring a considerable enhancement in case of NLOS reception due to the absence of LOS signal. Hence, NLOS mitigation can be performed on the data processing stage [9]. Many scientific studies carried out on NLOS mitigation at the level of antenna and hardware design, receiver, using either robust estimation [10], MP modeling [11] or by hybridizations with other external sensors. However, the class of robust estimation methods is generally characterized with a low breakdown point. A breakdown point is the proportion of outliers in the data that the estimator can handle before giving an arbitrarily large result.

Since LOS signals may be too scarce in urban environment, a new trend of techniques has recently received some attention in the literature. These methods aim to detect degraded measurements and use them constructively [4, 6] instead of eliminating them. In fact, under the poor conditions of satellites visibility, it is more interesting to use constructively these NLOS observables. Among the scientific studies in this field, the idea of using aiding information about the geometric environment of reception from 3D city models have been received a considerable interest [8]. These techniques aim to improve the measurements model for degraded measurement characterization. We can distinguish between methods using the simple information of 3D mapping and methods based on GNSS propagation simulation. The former type of method is based on predicting the path delay of the NLOS signals across an array of candidate positions [6, 13], i.e. considering signal reception at multiple candidate positions. The positioning technique is then based on scoring position hypotheses by comparison between the received observations at the receiver and ones of the information provided by 3D models such as the sky visibility [1], the NLOS signal delay [6], the PR measurements [13]. Others approaches combine a simplified 3D model, called urban trench, with a probabilistic method to enhance performances [14].

The second type of 3D-methods uses a 3D city model and a GNSS propagation simulator to predict the NLOS bias via and then correcting it in the PR measurements [4, 6]. 3D model jointly with a GNSS simulator to characterize on-the-fly the measurements errors in urban environments and to predict blockage and reflection of GNSS signals. GNSS simulators simulate the GNSS propagation in representative type of environments (e.g. open sky, urban and deep urban) and provide the user with several types of information such as the number and the characteristics of reflections, additional PR biases, etc. In [6], we have used the 3D model to predict PR errors and use it constructively on the estimation step. We have used these biases prediction in different ways, including instantaneous corrections, using the mean and variance, and other statistics such as the minimum and maximum bounds as constraints in the estimation process.

This constructive use of degraded measurements by PR correction is a sensitive task: poor PR biases prediction may engender an erroneous ranging correction and then may sensitively reduce the position estimation instead of enhancing it if the compensation term is not accurate enough. Another problem of 3D based methods is the computational loads and the high complexity. In fact, these approaches become computationally intensive if the search area is large. In this work, we propose an alternative to this 3D GNSS simulator. We investigate in an estimator that can jointly estimate the bias and the user position. We use constructively this bias estimate to correct PR measurements and enhance accuracy. Since the number of unknown of such problem exceeds generally the number of available signals, this inverse problem is said to be ill-posed and the observation matrix have generally a large condition number. One way to overcome this limitation is to found a sub-optimal solution with good proprieties of efficiency. In this study, we propose to originally use the framework of the regularization estimation which, to the best of our knowledge, has not been used before in the GNSS field.

Recently, there has been increased interest in regularized estimation in the robust statistics community. Among these studies, the τ estimator has been proposed in [19] to solve ill-conditioned linear inverse problems with outliers. This class of robust estimators is known to be simultaneously efficient and robust with a high breakdown point, i.e. they can handle a considerable proportion of outliers. Efficiency is provided in case of the estimator is well tuned. This estimator tuning in the case of GNSS signals is the main contribution of this study. We characterize the optimal condition that the regularization matrix of the estimation must verify to minimize the Mean Square Errors (MSE). We derivate also a new condition on this regularization matrix to realize the best trade-off of between estimation efficiency and stability. This condition is constructed by the minimizing the total MSE, i.e. the trace of the Mean Square Error matrix MSE. Finally, the proposed contributions are evaluated using real GNSS data from an urban canyon environment. Experimental results show that the proposed methods outperform robust estimation method in harsh environment with mixed NLOS and MP receptions.

Regularization algorithms have been used hitherto for solving ill-conditioned problems related to GNSS. [20] have investigated the use of an optimal Tikhonov-Phillips regularization method applied to carrier phase measurements to redress the problem of the GPS phase ambiguity resolution. Multipath Estimation and mitigation is performed using a truncated singular value decomposition (TSVD) regularization with ill-conditioning diagnosis at the RF signal level in [21]. But, the use of regularization methods in the domain of GNSS-based multipath and NLOS mitigation at the measurements level has not been widely studied. In this regard, this paper presents a relatively fresh perspective.

III. PROPOSED POSITIONING ALGORITHMS

A. *Problem Formulation*

GNSS is a satellite radionavigation system based on a constellation of satellites broadcasting specific spread-spectrum signals. Any civil user equipped with a dedicated GNSS receiver is able to estimate the time of travel of emitted signals along line-of-sight (LOS) paths from at least four satellites. However, signal obstruction and degradation are more prominent in harsh environments as oppose to open-sky areas, inducing then an additional MP/NLOS bias. Considering *N* emitting GNSS satellites, the following linearized equation formulates the satellite positioning problem [15]:

$$\mathbf{y} = \mathbf{H_0 x} + \mathbf{b} + \mathbf{v} \tag{1}$$

Where, throughout this paper, $\mathbf{x} = [x, y, z, b_c]^{\mathrm{T}}$ is the [*M*, 1] state vector containing the parameters of primary interest, i.e. the three coordinates of the user position (x, y, z) and the receiver clock bias b_c. $\mathbf{y}$ is the [*N*, 1] PR measurements vector. $\mathbf{H_0}$ contains the unit line-of-sight vectors between satellites and previous user position, $\mathbf{b}$ refers to the additional measurement bias caused by MP/NLOS receptions, commonly called as PR bias. $\mathbf{v}$ is the measurement noise. Traditionally, this latest term is supposed to be a white Gaussian noise characterized by a covariance matrix $\mathbf{R} = E\{\mathbf{vv}^{\mathrm{T}}\}$.

The distribution of the total noise $\mathbf{b}+\mathbf{v}$ is far from idealistic Gaussian model especially in harsh environments with many outliers. In this case, the latest distribution tends to be heavy tailed. Owing to the lack of prior information on MP/NLOS bias, weighted least-squares (WLS) estimation is usually used to estimate the user position:

$$\hat{\mathbf{x}}_{WLS} = \mathbf{H}_0^{+}\mathbf{y} \tag{2}$$

where $\mathbf{H}_0^{+} = (\mathbf{H}_0^{\mathrm{T}}\mathbf{R}^{-1}\mathbf{H}_0)^{-1}\mathbf{H}_0^{\mathrm{T}}\mathbf{R}^{-1}$ is the pseudo-inverse of $\mathbf{H_0}$ weighted by the inverse of covariance matrix $\mathbf{R}$.

The attractiveness of this WLS approach stems from its ease of implementation. However, the presence of MP/NLOS bias prevents this estimation from achieving good positioning performance since the Overall Mean Square Error (OMSE) of this estimation can be written as:

$$\begin{aligned} OMSE[\hat{\mathbf{x}}_{WLS}] &= tr\{MSE[\hat{\mathbf{x}}_{WLS}]\} \\ &= tr\left\{(\mathbf{H}_0^{\mathrm{T}}\mathbf{R}^{-1}\mathbf{H}_0)^{-1}\right\} + tr\left\{\mathbf{H}_0^{+}E\{\mathbf{bb}^{T}\}\left(\mathbf{H}_0^{+}\right)^{\mathrm{T}}\right\} \end{aligned} \tag{3}$$

Hence, estimating the parameter of interest $\mathbf{x}$ is not efficient without any information on the nuisance parameter $\mathbf{b}$. In this paper, we reformulate the classical problem (1) to consider a new state combing both parameter of interest and nuisance parameter. We modify the problem (1) to the following augmented problem:

$$\mathbf{y} = \mathbf{H}_1\mathbf{x}_1 + \mathbf{v} \tag{4}$$

Where $\mathbf{H}_1 = [\mathbf{H}_0, \mathbf{I}]$ and $\mathbf{x}_1 = (\mathbf{x}, \mathbf{b})^{\mathrm{T}}$ is the state vector to be estimated. We can notice that the state vector contains *N+M* unknowns and hence more that the available measurements $\mathbf{y}$. The inverse problem (4) is then ill-posed.

Another way to verify that this problem is ill-posed is to compute the condition number of the observation matrix $\mathbf{H}_1$:

$$cond(\mathbf{H}_1) = \sqrt{cond(\mathbf{H}_1^{\mathrm{T}}\mathbf{H}_1)}$$

By computing $\mathbf{H}_1^{\mathrm{T}}\mathbf{H}_1 = \begin{bmatrix} \mathbf{H}_0^{\mathrm{T}}\mathbf{H}_0 & \mathbf{H}_0^{\mathrm{T}} \\ \mathbf{H}_0 & \mathbf{I} \end{bmatrix}$, we can verify that this matrix is a singular matrix since:

$$\det(\mathbf{H}_1^{\mathrm{T}}\mathbf{H}_1) = \det(\mathbf{H}_0^{\mathrm{T}}\mathbf{H}_0 - \mathbf{H}_0^{\mathrm{T}}\mathbf{H}_0) = 0$$

This implies that the condition of the previous matrix is large and then: $cond(\mathbf{H}_1) = \sqrt{cond(\mathbf{H}_1^{\mathrm{T}}\mathbf{H}_1)} = \infty$. This result will be verified using real GNSS measurements in the experimental section. As detailed in [10], maximum-likelihood joint estimation of the position $\mathbf{x}$ and the bias $\mathbf{b}$ is impossible since the problem is ill-posed and overparameterized.

B. Regularized Position estimation

In case of an observation matrix with a large condition number, regularized robust estimation has been widely used in the literature to solve these ill-conditioned linear inverse problems [17, 18]. The regularization estimation aims to stabilize the parameters estimation by adding additional a priori information in the problem. Therefore, we propose to use the well-known regularization solution:

$$\hat{\mathbf{x}}_{\mathbf{T}} = \left(\mathbf{H}_1^{\mathrm{T}}\mathbf{H}_1 + \mathbf{T}\right)^{-1}\mathbf{H}_1^{\mathrm{T}}\mathbf{y} = \mathbf{A}_{\mathbf{T}}^{-1}\mathbf{H}_1^{\mathrm{T}}\mathbf{y} \tag{5a}$$

Where $\mathbf{A_T} = \mathbf{H}_1^{\mathrm{T}}\mathbf{H}_1 + \mathbf{T}$ and $\mathbf{T} = \begin{pmatrix} \mathbf{T}_1 & \mathbf{0} \\ \mathbf{0} & \mathbf{T}_2 \end{pmatrix}$ is a positive define square matrix. We note also $\mathbf{A}_0 = \mathbf{H}_1^{\mathrm{T}}\mathbf{H}_1$. We are aware that forcing the joint estimate of position and bias to have a particular form, i.e. belong to the family of regularized solution, is restricting the estimation of these parameters. In this work, we characterize and design a sub-optimal estimator of $\mathbf{x}$ and $\mathbf{b}$ that have the proprieties of efficiency and robustness, when it is well tuned.

The expression in (5a) is the solution of the following optimization problem:

$$\hat{\mathbf{x}}_{\mathbf{T}} = \arg\min_{\mathbf{z}}\left(\|\mathbf{y} - \mathbf{H}_1\mathbf{z}\|_2^2 + \|\mathbf{z}\|_{\mathbf{T}}^2\right) \tag{6}$$

Where $\|\mathbf{z}\|_{\mathbf{T}}^2 = \mathbf{z}^{\mathrm{T}}\mathbf{Tz}$ is the weighted norm of vector $\mathbf{z}$. This expression is also a quadratic cost function of the unknown to be estimated, as in the LS estimation. But, the additional second term allows adding an additional a priori knowledge into the statement of the initial problem. Choosing a “large” regularization matrix $\mathbf{T}$ will annihilate the effect of the first term, which indicates a high confidence that the linearized position, i.e. the previous user position, is close enough for the optimal solution. A “small” regularization matrix reflects high degree of uncertainty in the previous user position.

The regularization form using a regularization matrix $\mathbf{T}$ is a generalization of the oldest and well-known Tikhonov regularization technique [22] that assumes $\mathbf{T} = \gamma\mathbf{I}$, with $\gamma > 0$. $\mathbf{T}$ or γ are called the regularization matrix or parameter. When γ is high, the noise components will be filtered out with the proposed solution yielding an overly smooth estimation. On the other hand, a small value of γ induce an inadequate filtering of the noise which gives a highly oscillatory estimation. Then, this tuning regularization matrix $\mathbf{T}$ or parameter γ must be wisely chosen to optimize the estimation. This will be the object of the following sub-sections.

Finally, since $\mathbf{H}_1 = [\mathbf{H}_0, \mathbf{I}]$ and $\mathbf{x}_1 = (\mathbf{x}, \mathbf{b})^{\mathrm{T}}$, the regularization formulation is equivalent, in the particle case of GNSS, to a LS estimation with PR measurement correction using a bias estimation:

$$\hat{\mathbf{x}} = \left(\mathbf{H}_0^{\mathrm{T}}\mathbf{H}_0\right)^{-1}\mathbf{H}_0^{\mathrm{T}}\left(\mathbf{y} - (\mathbf{I}_N + \mathbf{T}_2)\hat{\mathbf{b}}\right) \tag{5b}$$

We consider now the Overall MSE defined as:

$$OMSE[\hat{\mathbf{x}}_\mathbf{T}] = tr\left\{E\left\{(\mathbf{x}_1 - \hat{\mathbf{x}}_\mathbf{T})(\mathbf{x}_1 - \hat{\mathbf{x}}_\mathbf{T})^\mathrm{T}\right\}\right\} \quad (7)$$

This OMSE can be simply expressed as:

$$\begin{aligned} OMSE[\hat{\mathbf{x}}_\mathbf{T}] &= tr\left\{(\mathbf{A}_\mathbf{T}^{-1}\mathbf{H}_1^\mathrm{T}\mathbf{R}\mathbf{H}_1\mathbf{A}_\mathbf{T}^{-1})\right\} + \\ & tr\left\{E\left\{(\mathbf{A}_\mathbf{T}^{-1}\mathbf{A}_0 - \mathbf{I})\mathbf{x}_1\mathbf{x}_1^\mathrm{T}(\mathbf{A}_0\mathbf{A}_\mathbf{T}^{-1} - \mathbf{I})\right\}\right\} \end{aligned} \quad (8)$$

The first term in (8) denotes the regularized estimate variance and depends on the noise covariance matrix. The second term represents the squared norm of the bias of the regularization estimation and depends on the unknown parameters $\mathbf{x}_1$.

Note that $(\mathbf{I} - \mathbf{A}_\mathbf{T}^{-1}\mathbf{A}_0) = \mathbf{A}_\mathbf{T}^{-1}\mathbf{T}$ and $(\mathbf{I} - \mathbf{A}_0\mathbf{A}_\mathbf{T}^{-1}) = \mathbf{T}\mathbf{A}_\mathbf{T}^{-1}$, expression (8) can be simplified to:

$$OMSE[\hat{\mathbf{x}}_\mathbf{T}] = tr\left\{\mathbf{A}_\mathbf{T}^{-2}\left(\mathbf{T}\mathbf{C}_{\mathbf{x}_1}\mathbf{T} + \mathbf{H}_1^\mathrm{T}\mathbf{R}\mathbf{H}_1\right)\right\} \quad (9)$$

Where $\mathbf{C}_{\mathbf{x}_1} = E\left\{\mathbf{x}_1\mathbf{x}_1^\mathrm{T}\right\}$ is the covariance matrix of the unknown $\mathbf{x}_1$. Since the parameter of interest $\mathbf{x}$ is determinist, this covariance matrix is equal to:

$$\mathbf{C}_{\mathbf{x}_1} = E\left\{\mathbf{x}_1\mathbf{x}_1^\mathrm{T}\right\} = \begin{pmatrix} \mathbf{0} & \mathbf{0} \\ \mathbf{0} & \mathbf{C}_\mathbf{b} = E\left\{\mathbf{b}\mathbf{b}^\mathrm{T}\right\} \end{pmatrix}$$

Another classical approximation is generally used is to assume that measurement noise components are independent and with equal variance, i.e. $\mathbf{R} = E\left\{\mathbf{v}\mathbf{v}^\mathrm{T}\right\} = \sigma_v^2\mathbf{I}$. This yield:

$$OMSE[\hat{\mathbf{x}}_\mathbf{T}] = tr\left\{\mathbf{A}_\mathbf{T}^{-2}\left(\mathbf{T}\mathbf{C}_{\mathbf{x}_1}\mathbf{T} + \sigma_v^2\mathbf{A}_0\right)\right\} \quad (10)$$

In the following sub-sections, we will derive the optimal regularization estimation to define the optimal regularization matrix $\mathbf{T}$ under accuracy criterion, with and without constraints on the estimate $\hat{\mathbf{x}}_\mathbf{T}$.

C. Proposed Optimized Regularized Position estimation

1) Optimal Regularization Matrix Derivation

In this sub-section, we derive a regularized least-squares solution that optimizes the solution accuracy by minimizing the overall MSE defined in (10). This implies finding the optimal regularization matrix minimizing the overall MSE as:

$$\mathbf{T}_{opt} = \mathbf{T}_{acc} = \arg\min_{\mathbf{T}}(OMSE[\hat{\mathbf{x}}_\mathbf{T}]) \quad (11)$$

By deriving the overall MSE expression (10), we get, in the case of this condition (*) $\mathbf{T}_1 = \mathbf{H}_0^\mathrm{T}\left(\mathbf{H}_0\mathbf{H}_0^\mathrm{T}\right)^{-1}\mathbf{T}_2\mathbf{H}_0$:

$$\frac{\partial\, OMSE[\hat{\mathbf{x}}_\mathbf{T}]}{\partial\mathbf{T}} = 2\left(\mathbf{T}\mathbf{C}_\mathbf{x} - \sigma_v^2\mathbf{I}\right)\mathbf{A}_\mathbf{T}^{-3}\mathbf{A}_0 \quad (12)$$

Proof: See Appendix A.

The condition (*) $\mathbf{T}_1 = \mathbf{H}_0^\mathrm{T}\left(\mathbf{H}_0\mathbf{H}_0^\mathrm{T}\right)^{-1}\mathbf{T}_2\mathbf{H}_0$ must be verified to get the previous expression as explained in the appendix A. Hence, without loss of generality, we can impose this expression for the first term of the regularization matrix $\mathbf{T}$. We can easily verify that in the case of Tikhonov regularization ($\mathbf{T} = \gamma\mathbf{I}$), the condition (*) is verified.

By setting the previous expression to zero, we find the expression of the optimal regularization matrix:

$$\mathbf{T}_{acc} = \sigma_v^2\mathbf{D}_1 \Leftrightarrow \begin{cases} \mathbf{T}_1 = \left(\mathbf{H}_0^\mathrm{T}\mathbf{H}_0\right)^{-1}\mathbf{H}_0^\mathrm{T}\mathbf{T}_2\mathbf{H}_0 \\ \mathbf{T}_2 = \sigma_v^2\mathbf{C}_\mathbf{b}^{-1} \end{cases} \quad (13)$$

Where $\mathbf{D}_1 = \begin{pmatrix} \left(\mathbf{H}_0^\mathrm{T}\mathbf{H}_0\right)^{-1}\mathbf{H}_0^\mathrm{T}\mathbf{C}_\mathbf{b}^{-1}\mathbf{H}_0 & \mathbf{0} \\ \mathbf{0} & \mathbf{C}_\mathbf{b}^{-1} \end{pmatrix}$. This result is also in agreement with the result found in [17] in the simplified case of a Tikhonov regularization technique: $\mathbf{T} = \gamma\mathbf{I}$, except that we treat an augmented problem in this paper. In this case, the optimal regularization parameter will be equal to:

$$\gamma_{opt} = \sigma_\mathbf{b}^{-2}\sigma_v^2 \quad (14)$$

Where $\sigma_\mathbf{b}^2$ represents the mean value of the diagonal elements of the bias covariance matrix, i.e. $\sigma_\mathbf{b}^2 = Mean(diag(\mathbf{C}_\mathbf{b}))$.

Since the defined optimal regularization matrix in (13) depends on $\mathbf{C}_\mathbf{b}^{-1}$ and from the expression of the position estimation (5b), we can see that this form will reduce the effect of contaminated signals on the final regularization least-squares estimation and hence improve the final position estimation: degraded satellites having huge MP/NLOS biases will be more corrected than potentially healthy satellites having low MP/NLOS biases.

Throughout this paper, this proposed approach with the optimal regularization matrix will be called the Augmented Regularized Least Squares (ARLS) solution.

2) Theoretical Performance of ARLS

For the expression (13) of the optimal regularization matrix, and using the expression of the OMSE in (9), the minimum OMSE is equals to:

$$OMSE[\hat{\mathbf{x}}_\mathbf{T}]_{Min} = tr\left\{\sigma_v^2\mathbf{A}_{\mathbf{T}_{acc}}^{-1}\right\} = \sigma_v^2 tr\left\{\left(\mathbf{A}_0 + \sigma_v^2\mathbf{D}_1\right)^{-1}\right\} \quad (15)$$

According to (15), the maximal accuracy performance by regularized estimation can be expressed, using Blockwise inversion, as:

$$OMSE\ [\hat{\mathbf{x}}_\mathbf{T}]_{Min} = \sigma_v^2\left(tr\{\mathbf{M}_0\} + tr\{\mathbf{M}_1\}\right) \quad (16)$$

Where $\mathbf{M}_0 = \left(\mathbf{H}_0^\mathrm{T}\mathbf{H}_0 + \mathbf{T}_1 - \mathbf{H}_0^\mathrm{T}(\mathbf{I}_N + \mathbf{T}_2)^{-1}\mathbf{H}_0\right)^{-1}$ and $\mathbf{M}_1 = (\mathbf{I}_N + \mathbf{T}_2)^{-1} + (\mathbf{I}_N + \mathbf{T}_2)^{-1}\mathbf{H}_0\mathbf{M}_0\mathbf{H}_0^\mathrm{T}(\mathbf{I}_N + \mathbf{T}_2)^{-1}$. This expression of OMSE represents overall error of the joint estimation of the user position and the MP/NLOS bias.

By linearity of the trace operator and after some algebraic manipulations, relation (16) can be expressed also as:

$$OMSE[\hat{\mathbf{x}}_\mathbf{T}]_{Min} = \sigma_v^2\begin{pmatrix} tr\left\{(\mathbf{I}_N + \mathbf{T}_2)^{-1}\right\} + \\ tr\left\{\left(\mathbf{I}_M + \mathbf{H}_0^\mathrm{T}(\mathbf{I}_N + \mathbf{T}_2)^{-2}\mathbf{H}_0\right)\mathbf{M}_0\right\} \end{pmatrix} \quad (17)$$

In the case of Tikhonov regularization, i.e. $\mathbf{T}_2 = \gamma_{opt}\mathbf{I}_N$ and $\mathbf{T}_1 = \gamma_{opt}\mathbf{I}_M$, the previous expression can be simplified on:

$$OMSE[\gamma_{opt}]_{Min} = \frac{\sigma_v^2\left(N\gamma_{opt} + M\right)}{\gamma_{opt}\left(\gamma_{opt} + 1\right)} + \sigma_v^2 tr\left\{\left(\mathbf{H}_0^\mathrm{T}\mathbf{H}_0 + (\gamma_{opt} + 1)\mathbf{I}_M\right)^{-1}\right\} \quad (18)$$

Proof: See Appendix B.

We can immediately verify that $OMSE\lfloor\gamma_{opt}\rfloor_{Min}$ is monotonically decreasing in γ_{opt}. In the case of high degraded measurements, i.e. a large bias covariance matrix $\mathbf{C_b}$, $\gamma_{opt} \to 0$, hence, $OMSE\lfloor\gamma_{opt}\rfloor_{Min} \to \infty$. This result is coherent with reality since, unfortunately, large bias covariance matrix $\mathbf{C_b}$ represents the case of high bias to signal ratio and hence any estimator will not be able to estimate the parameter of interest $\mathbf{x}$ since the nuisance parameter $\mathbf{b}$ is so large, i.e. very degraded measurements. In the case of unhealthy measurements, i.e. a small bias covariance matrix $\mathbf{C_b}$, $\gamma_{opt} \to \infty$, hence, $OMSE\left[\gamma_{opt}\right]_{Min} \to \sigma_v^2 tr\left\{(\mathbf{H}_0^{\mathrm{T}}\mathbf{H}_0)^{-1}\right\}$. This limit represents the minimal OMSE of problem (1) in case of free-bias, i.e. $\mathbf{b} = 0$.

We compare the theoretical performance of bias estimation of this augmented regularized LS with the performance of the conventional LS. The minimal error on position estimation by ARLS is equals to:

$$OMSE[\hat{\mathbf{x}}]_{Min} = tr\left\{\sigma_v^2 \mathbf{W}\mathbf{A}_{\mathbf{T}_{acc}}^{-1}\right\} = \sigma_v^2 tr\{\mathbf{M}_0\} \quad (19)$$

Where the weighting matrix $\mathbf{W} = \begin{pmatrix} \mathbf{I}_M & \mathbf{0} \\ \mathbf{0} & \mathbf{0} \end{pmatrix}$ is used to express the individual error on the position estimation. In the case of Tikhonov regularization, i.e. $\mathbf{T}_2 = \gamma_{opt}\mathbf{I}_N$ and $\mathbf{T}_1 = \gamma_{opt}\mathbf{I}_M$, and using equation (14), the minimal error on position estimation can be related to the mean bias covariance:

$$OMSE[\hat{\mathbf{x}}]_{Min} = \frac{\sigma_v^2\left(\sigma_{\mathbf{b}}^{-2}\sigma_v^2 + 1\right)}{\sigma_{\mathbf{b}}^{-2}\sigma_v^2} tr\left\{\left(\mathbf{H}_0^{\mathrm{T}}\mathbf{H}_0 + \left(\sigma_{\mathbf{b}}^{-2}\sigma_v^2 + 1\right)\mathbf{I}_M\right)^{-1}\right\} \quad (20)$$

From (3), the Overall Mean Square Error of the WLS estimation (2) can be written as, in the case of $\mathbf{C_b} = \sigma_{\mathbf{b}}^2\mathbf{I}_N$:

$$OMSE[\hat{\mathbf{x}}_{WLS}] = \frac{\sigma_v^2\left(\sigma_{\mathbf{b}}^{-2}\sigma_v^2 + 1\right)}{\sigma_{\mathbf{b}}^{-2}\sigma_v^2} tr\left\{(\mathbf{H}_0^{\mathrm{T}}\mathbf{H}_0)^{-1}\right\} \quad (21)$$

The difference on OMSE between ARLS and WLS is:

$$OMSE[\hat{\mathbf{x}}]_{Min} - OMSE[\hat{\mathbf{x}}_{WLS}] = \frac{\sigma_v^2\left(\sigma_{\mathbf{b}}^{-2}\sigma_v^2 + 1\right)}{\sigma_{\mathbf{b}}^{-2}\sigma_v^2} \times \left[tr\left\{\left(\mathbf{H}_0^{\mathrm{T}}\mathbf{H}_0 + \left(\sigma_{\mathbf{b}}^{-2}\sigma_v^2 + 1\right)\mathbf{I}_M\right)^{-1}\right\} - tr\left\{(\mathbf{H}_0^{\mathrm{T}}\mathbf{H}_0)^{-1}\right\}\right] \quad (22)$$

Since the last term of relation (22) is always negative, this relation proves that for any level of MP/NLOS bias $\sigma_{\mathbf{b}}$, the proposed ARLS estimator will outperform the WLS estimator.

Finally, we can verify that the minimal error on position estimation using ARLS, $OMSE[\hat{\mathbf{x}}]_{Min}$ given in (20), is monotonically decreasing in $\sigma_{\mathbf{b}}$ and is majored by the minimal OMSE of problem (1), corresponding to the case of free-bias $\mathbf{b} = 0$, which is equals to:

$$OMSE_{Min} = \sigma_v^2 tr\left\{(\mathbf{H}_0^{\mathrm{T}}\mathbf{H}_0)^{-1}\right\} \quad (23)$$

D. Pratical Implementation of the proposed algorithm

1) MP/NLOS bias covariance matrix

The found constrained optimal regularization matrix in (13) depends on the observation matrix and PR measurements. The only unknown on the found expression is the covariance matrix of the MP/NLOS bias $\mathbf{C_b}$. This covariance matrix can be deduced using a prior distribution on the bias, by modeling PR bias, as it is done in [11].

For the sake of simplicity to apply the regularized estimation approach, we assume in this work that MP-NLOS biases are zero-mean Gaussian distributed with a variance following an C/N0-Elevation model, i.e. each noise variance is linked to the satellite elevation angle and signal to noise ratio with the following:

$$\sigma_i^2 = \frac{k \times 10^{-\left(\frac{(CN0)_i}{10}\right)}}{\sin^2(\theta_i)}$$

We have used the C/N0-Elevation model proposed in [2]. Hence, we have, $\mathbf{C_b} = diag(\sigma_i^2)_{i=1,..,N}$. The factor k is taken equal to $k = \sigma_v^2 10^{0.1 \times (CN0)_{Max}}$. Other bias models could be applied and analyzed.

2) Augmented Regularized Least Squares:

From the expression of the regularization matrix $\mathbf{T} = \begin{pmatrix} \mathbf{T}_1 & \mathbf{0} \\ \mathbf{0} & \mathbf{T}_2 \end{pmatrix}$ and the condition $\mathbf{T}_1 = \mathbf{H}_0^{\mathrm{T}}\left(\mathbf{H}_0\mathbf{H}_0^{\mathrm{T}}\right)^{-1}\mathbf{T}_2\mathbf{H}_0$, we deduce that the basic hypothesis on the regularization matrix, i.e. a positive define square matrix, doesn't hold in the case where *N≤M,* i.e. in the case where the number of unknowns (*M*) exceed the number of available PR measurements (*N*). In this situation, the condition number of the matrix $\mathbf{H}_0\mathbf{H}_0^{\mathrm{T}}$ become infinite and the regularization matrix $\mathbf{T}$ is singular.

To overcome this limitation, we can simply notice that in the case of Tikhonov regularization $\mathbf{T}_2 = \gamma\mathbf{I}_N$ and then the condition (*) can be written as: $\mathbf{T}_1 = \gamma\mathbf{I}_M$. In this case, the regularization matrix $\mathbf{T} = \begin{pmatrix} \mathbf{T}_1 & \mathbf{0} \\ \mathbf{0} & \mathbf{T}_2 \end{pmatrix}$ is nonsingular and the regularization estimation can be performed. We propose then to use the Tikhonov regularization only in the case where *N≤M,* otherwise we will use the optimal regularization matrix form found in (13). The following scheme resumes the proposed ARLS approach for bias and position estimation.

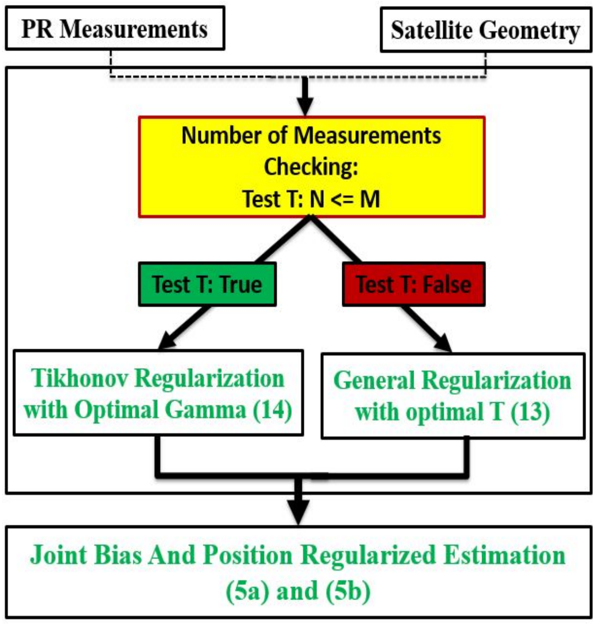

Fig 1. Scheme of the proposed ARLS

3) Augmented Regularized EKF:

A huge amount of GNSS applications in urban environment addresses vehicles moving slowly in a dense urban area. Hence, we aim to modify our algorithm with a second-order model to describe the dynamic of the vehicle in the GNSS earth-centered earth-fixed (ECEF) frame. The state vector will contain three parts which are the position, the velocity of the vehicle in the ECEF frame and the MP/NLOS bias vector:

$$\mathbf{x}_2 = (x, \dot{x}, y, \dot{y}, z, \dot{z}, b_c, d_c, \mathbf{b})^{\mathrm{T}}$$

Where $\mathbf{x} = [x, y, z, b_c]^{\mathrm{T}}$ are the vehicle position (x, y, z) and b_c the receiver clock bias. $\dot{\mathbf{x}} = [\dot{x}, \dot{y}, \dot{z}, d_c]^{\mathrm{T}}$ represents the vehicle velocity $(\dot{x}, \dot{y}, \dot{z})$ and the GNSS receiver clock drift.

We adopt a random walk for the velocity model, i.e. we assume that the second derivate of the position $(\ddot{x}, \ddot{y}, \ddot{z})$ is a zero mean Gaussian noise $\mathbf{n}_x$ with a known variance $\sigma_{n_x}^2$. The receiver clock bias and drift can also be modelled as random walks such as: $\dot{b}_c = d_c + e_b$ and $\dot{d}_c = e_d$ where e_b and e_d are zero-mean Gaussian white noises of variances σ_b^2 and σ_d^2 .

Generally, there is no relation that rely two consecutive MP/NLOS bias vectors. Based on the above assumptions, we can describe the state propagation between two-time epochs *k* and *k+1* as:

$$(\mathbf{x}_2)_{k+1} = \mathbf{\Phi}_{k+1|k} (\mathbf{x}_2)_k + \mathbf{n}_k \quad (24)$$

Where $\mathbf{n}_k = [\mathbf{n}_x, e_b, e_d, \mathbf{0}_{1\times N}]^{\mathrm{T}}$ is the zero-mean Gaussian white vector with a covariance matrix $\mathbf{Q}_k = \begin{pmatrix} \mathbf{Q}_k^X & \mathbf{0} & \mathbf{0} \\ \mathbf{0} & \mathbf{Q}_k^V & \mathbf{0} \\ \mathbf{0} & \mathbf{0} & \mathbf{0} \end{pmatrix}$.

The block-diagonal state matrix $\mathbf{\Phi}_{k+1|k}$ can be expressed as:

$$\mathbf{\Phi}_{k+1|k} = \begin{pmatrix} \mathbf{\Phi}_k^X & \mathbf{0} & \mathbf{0} \\ \mathbf{0} & \mathbf{\Phi}_k^V & \mathbf{0} \\ \mathbf{0} & \mathbf{0} & \mathbf{0} \end{pmatrix}$$

The different block matrices can be defined as follows:

$$\mathbf{\Phi}_k^X = \begin{pmatrix} \mathbf{\Phi}_k^V & \mathbf{0} & \mathbf{0} \\ \mathbf{0} & \mathbf{\Phi}_k^V & \mathbf{0} \\ \mathbf{0} & \mathbf{0} & \mathbf{\Phi}_k^V \end{pmatrix}; \ \mathbf{\Phi}_k^V = \begin{pmatrix} 1 & \Delta t \\ 0 & 1 \end{pmatrix}$$

$$\mathbf{Q}_k^X = \begin{pmatrix} \mathbf{M}_k^X & \mathbf{0} & \mathbf{0} \\ \mathbf{0} & \mathbf{M}_k^X & \mathbf{0} \\ \mathbf{0} & \mathbf{0} & \mathbf{M}_k^X \end{pmatrix}; \ \mathbf{M}_k^X = \sigma_{n_x}^2 \begin{pmatrix} \Delta t^4/4 & \Delta t^3/4 \\ \Delta t^3/2 & \Delta t^2 \end{pmatrix};$$

$$\mathbf{Q}_k^V = \begin{pmatrix} \sigma_b^2 \Delta t^2 + \frac{\sigma_d^2 \Delta t^4}{4} & \frac{\sigma_d^2 \Delta t^3}{4} \\ \frac{\sigma_d^2 \Delta t^3}{4} & \sigma_d^2 \Delta t^2 \end{pmatrix}$$

Δt represents the time sampling, i.e. time interval between two successive samples.

By combining the propagation formulation (24) and the relation (5b), we develop a regularized extended Kalman Filter (EKF) solution as an extended Kalman filter applied to corrected PR measurements using a bias estimation. If we note EKF the conventional EKF solution then the proposed regularized EKF can be formulated as:

$$\begin{cases} \begin{bmatrix} - \\ \hat{\mathbf{b}} \end{bmatrix} = \left(\mathbf{H}_1^{\mathrm{T}} \mathbf{H}_1 + \mathbf{T}\right)^{-1} \mathbf{H}_1^{\mathrm{T}} \mathbf{y} \\ \hat{\mathbf{x}} = EKF\left(\mathbf{y} - (\mathbf{I}_N + \mathbf{T}_2)\hat{\mathbf{b}}\right) \end{cases} \quad (25)$$

To summarize, we propose in this study two different versions of optimized augmented regularized solution: an Augmented Regularized Least Squares (ARLS), an Augmented Regularized EKF (AREKF). For way of illustration, the AREKF algorithm is summarized below. For the ARLS algorithm, the approach is similar, except omitting the user dynamic.

Algorithm: AREKF

Input: $\mathbf{y}$, $\mathbf{H_0}$

{Initialization: Conventional LS for some iteration}

% Compute the augmented matrix

Define the following matrix $\mathbf{H}_1 = [\mathbf{H}_0, \mathbf{I}]$, $\mathbf{A}_0 = \mathbf{H}_1^{\mathrm{T}} \mathbf{H}_1$

% Predict the bias covariance matrix using C/N0-Elevation model: $\mathbf{C_b} = diag(\sigma_i^2)_{i=1,..,N}$

% Compute the optimal regularization matrix $\mathbf{T}_{acc}$ using (13)

Test on the number of Satellites:

- *N≤M*, Compute $\mathbf{T}_{acc} = \gamma_{opt} \mathbf{I} = \sigma_{\mathbf{b}}^{-2} \sigma_v^2 \mathbf{I}$
- *N>M*, Compute $\mathbf{T}_{acc} = \sigma_v^2 \mathbf{D}_1$

Where $\sigma_{\mathbf{b}}^2 = \underset{i}{Mean}(\sigma_i^2)$

% Compute the regularized least squares to find an estimate of the bias and the final position as:

$$\begin{cases} \begin{bmatrix} - \\ \hat{\mathbf{b}}_{\text{AREKF}} \end{bmatrix} = \left(\mathbf{H}_1^{\mathrm{T}} \mathbf{H}_1 + \mathbf{T}_{acc}\right)^{-1} \mathbf{H}_1^{\mathrm{T}} \mathbf{y} \\ \hat{\mathbf{x}}_{\text{AREKF}} = EKF\left(\mathbf{y} - \left(\mathbf{I}_N + (\mathbf{T}_2)_{acc}\right)\hat{\mathbf{b}}_{\text{AREKF}}\right) \end{cases}$$

Output: $\hat{\mathbf{x}}_{\text{AREKF}}$, $\hat{\mathbf{b}}_{\text{AREKF}}$

IV. Experimental Results

A. General Experimental Setup

To evaluate the proposed technique, a dynamic positioning test was conducted in an urban environment along the “Capitole Square” in Toulouse. PR measurements, comprising GPS and GLONASS, were recorded using an AsteRx3 SEPTENTRIO receiver, and a SPAN Novatel system including a DGPS receiver tightly integrated with an IMU-FSAS (from iMAR), both at a rate of 10 Hz. Trajectory provided by the Novatel system is considered as reference trajectory.

For this validation test, we use a 3-min trajectory along an urban environment characterized by narrow streets and tall buildings, which are predominantly the down-towns of European cities. The following table summarizes the set of some of the received GPS/GLONASS signals during this measurement campaign. We use the algorithm proposed in [16] for true bias estimation.

TABLE I. SOME RECEIVED SIGNALS IN THE CONSIDERED URBAN SECTION (G FOR GPS SATELLITES AND R FOR GLONASS SATELLITES)

	G12	G13	G15	G22	G28	R08	R09	R11
Elev. (°)	21.4	52.4	82.2	5.9	26	62	35	25.5
C/N_0 (*dB-Hz*)	33.5	42	47.7	35.5	27.7	34	24	28
Mean bias (m)	6.4	3	0	6.6	3.5	-0.6	3	-7.1
Maxi. bias (m)	15.9	11.5	0	33.2	23.9	-19.1	31.7	-19

An overview of the considered urban environment and the Sky-plot of the GPS and GLONASS received satellites in the deep urban section are shown in Fig. 2.

(a)

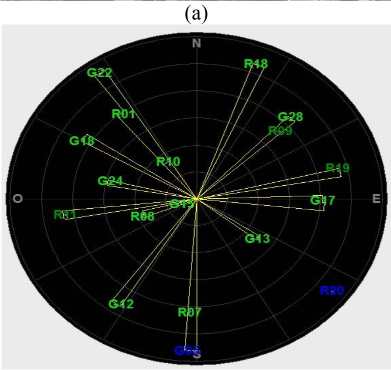

(b)

Fig 2. (2)a. Dynamic test in Toulouse. White line indicates the reference trajectory; (2)b. Sky-plot of GPS/GLONASS satellites

In this kind of environment, the use of more than one constellation is essential. Fig. 3 shows that by considering GLONASS constellation, we increase by a factor of two the number of available signals. This signal availability will improve the satellite visibility and their geometrical distribution which reduces the DOP and hence enhances the position estimation.

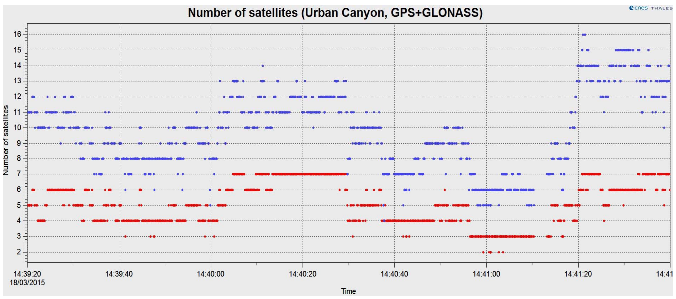

Fig 3. Number of used satellites: Blue color refers to GPS/GLONASS Satellites and red color refers to GPS Satellites.

Finally, the degradation in this environment is also clearly apparent at the received measurements level. As shown in Fig. 4, the signal to noise ratios of the received satellites present enormous fluctuations because of the interaction of these signal with the environment and the attenuation caused by reflections and diffractions.

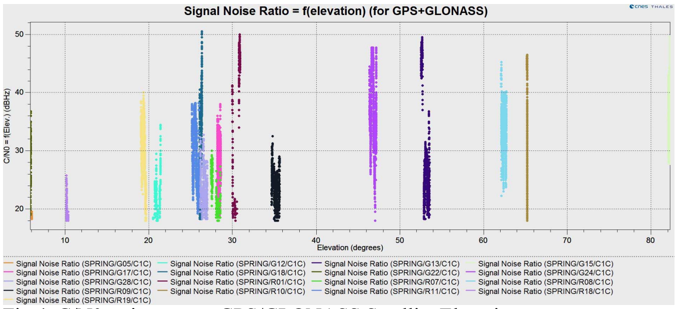

Fig 4. C/N0 ratios versus GPS/GLONASS Satellite Elevations

B. Condition Number of the Augmented Problem

In this sub-section, we validate the fundamental assumption of this study which is the ill-conditioning of the augmented observation matrix in problem (4). This result has justified the use of the regularization formulation in this study. Fig. 5 shows the condition number of the observation matrix $\mathbf{H}_1$ in the considered urban environment:

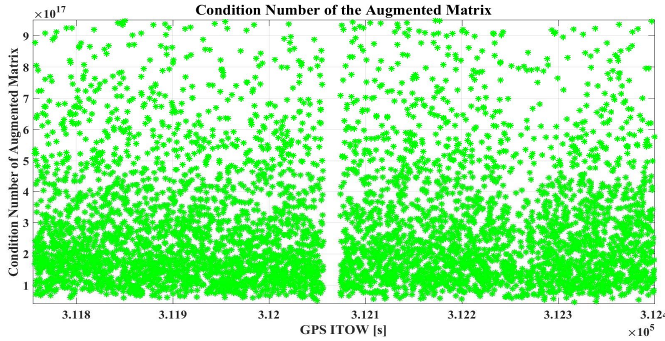

Fig 5. Condition number of the augmented observation matrix versus time

It is clearly apparent from the previous figure that the condition number of the augmented observation matrix $\mathbf{H}_1$ is infinite. This result is highlighted in the following table.

TABLE II. CONDITION NUMBER OF THE AUGMENTED MATRIX

	Mean	*Maximum*	*Minimum*
Condition Number of $\mathbf{H}_1$	1.7305e+18	1.7171e+21	4.6078e+16

C. Tikhonov Regularization Solution

In this sub-section, we evaluate the performance of the well-known Tikhonov regularization technique which is a particular case of our proposed algorithm by assuming $\mathbf{T} = \gamma \mathbf{I}$, where $\gamma > 0$ is the regularization parameter. First, we study the performance of ARLS and AREKF against a conventional least squares and a robust version of EKF [10] for different values of the regularization parameter γ. To analyze the trend, only GPS satellites are used on this first plot. Results are shown in Fig. 6:

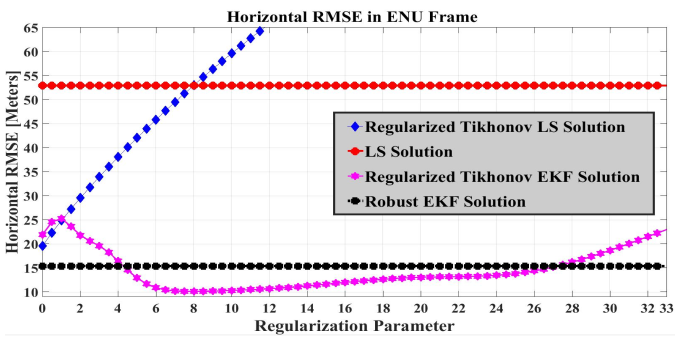

Fig 6. Horizontal RMSE of different solution estimation versus the regularization parameter γ

In this sub-section, we will evaluate the performance of the Augmented Regularized Least Squares (ARLS) and the Augmented Regularized EKF (AREKF) for this particular case of regularization matrix. From the third sub-section of section 3, we have the expression of the optimal regularization matrix and by substituting $\mathbf{T} = \gamma\mathbf{I}$, we get:

$$\gamma_{opt} = \sigma_{\mathbf{b}}^{-2}\sigma_{v}^{2}$$

We take $\sigma_{\mathbf{b}}^{2} = \underset{i}{Mean}(\sigma_{i}^{2}) \approx 9\sigma_{v}$, then $\gamma_{opt} = 9$. Following figures show the performance of the Augmented Regularized Least Squares (ARLS) and the Augmented Regularized EKF (AREKF) versus a robust Kalman Filter for different values of regularization parameter γ and for the optimal γ_{opt}. A value of $\gamma = 0.01$ have been taken for the Augmented Regularized Least Squares (ARLS) estimator.

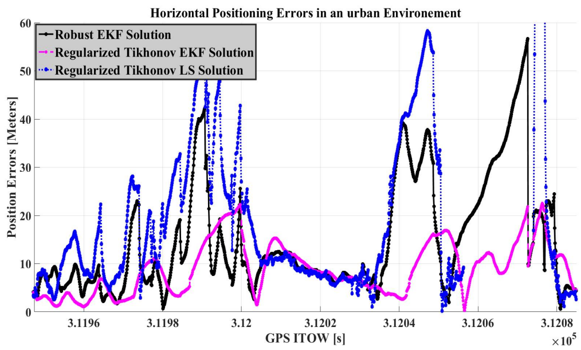

(a)

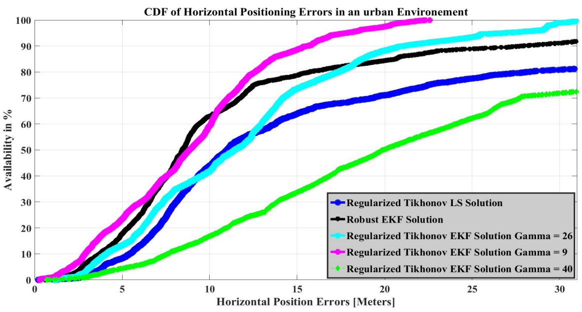

(b)

Fig 7. Horizontal Positioning Errors (HPE) of different solution estimation (7)a HPE versus time; (7)b CDF of HPE for different value of Gamma

The following table summarizes the horizontal positioning errors for these different estimators:

TABLE III. HORIZTONAL POSITIONING PERFORMANCES

	Robust EKF	Tikhonov ARLS	REKF (Tikhonov $\gamma = 9$)	REKF (Tikhonov $\gamma = 26$)	REKF (Tikhonov $\gamma = 40$)
H-RMSE [m]	11.8	15.2	8.86	12	25.8

Previous figures and table show clearly that the optimized AREKF outperform the other estimators for the optimal regularization parameter. When the regularization parameter γ tends to infinity, the solution tends to the null solution and then the positioning errors diverge.

We evaluate also the performance of the proposed algorithm on the bias estimation. We use the algorithm proposed in [16] for true bias estimation. In Fig. 8, we plot the difference between the absolute true bias and the absolute estimated bias for GPS satellites, i.e. we plot $\Delta\mathbf{b} = \left|\mathbf{b}_{True}\right| - \left|\hat{\mathbf{b}}_{\gamma=\gamma_{opt}}\right|$. $\mathbf{b}_{True}$ denotes the estimated true bias and $\hat{\mathbf{b}}_{\gamma=\gamma_{opt}}$ represents the estimated bias for $\gamma = \gamma_{opt}$. The following table gives the elevation angles of the set of GPS satellites used in Fig. 8.

TABLE IV. ELEVATION ANGLES OF THE RECEIVED GPS SATELLITES

GPS Satellites	**G12**	**G13**	**G15**	**G17**	**G18**	**G24**	**G28**
Elevation (°)	21	52	82	28	26	47	26

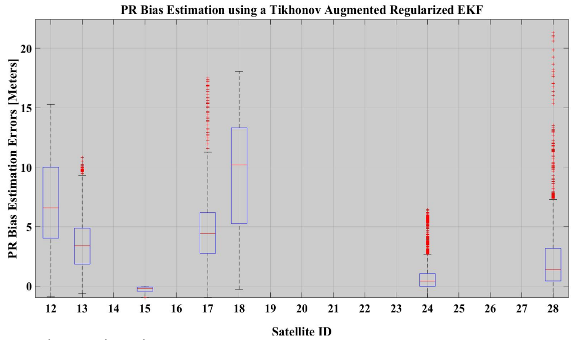

Fig 8. PR Bias Estimation Error

It is apparent from Fig. 8 that for high elevation satellites such as SV15 and SV24, the bias has been well estimated using the AREKF algorithm. We note also that $\Delta\mathbf{b}$ is almost all the time positive. This mean that the AREKF algorithm tends to underestimate the bias, which is a good aspect since overestimating the MP/NLOS bias can engender a great risk of deteriorating PR measurements instead of correcting them if the compensation term is not accurate enough and overestimated. Finally, that the overall error on bias estimation exceed rarely 5 meters in this considered scenario.

D. *Performances of the Optimal Regularization Estimation*

In this sub-section, we evaluate the performance of the proposed AREKF algorithm in both case of Tikhonov regularization with an optimal regularization parameter $\gamma > 0$ and in the general case with an optimal regularization matrix. Following figure shows the performance of the Augmented Regularized EKF (AREKF) for the optimal γ_{opt} and for the optimal $\mathbf{T}_{acc} = \sigma_{v}^{2}\mathbf{D}_{1}$, versus a robust Kalman Filter with a C/N0 thresholding. The threshold used for C/N0 is equals to 38 dB-Hz. We have used the same measurements set as the previous sub-section.

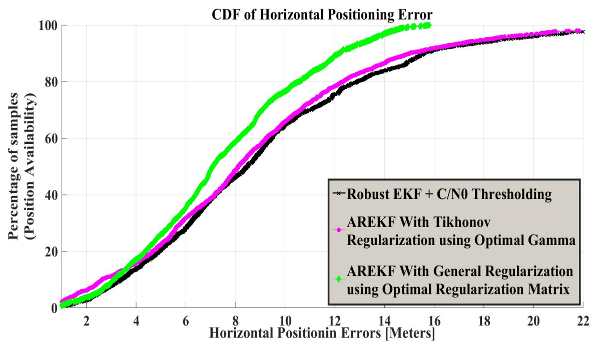

Fig 9. Horizontal Positioning Errors (HPE) of different solution

Previous figure shows that the optimized AREKF with a general regularization matrix outperform the optimized AREKF with Tikhonov regularization using the optimal γ_{opt} and the robust EKF. This method enhances both the mean estimation performance and the mitigation of large positioning errors or heavy-tailed errors.

The following table summarizes the horizontal positioning errors (HPE) and the Bias Estimation Errors (BEE) for these different estimators. The Bias Estimation Errors (BEE) is expressed as the Euclidean norm between the estimated bias and the true bias, computed using [16]:

TABLE V. HORIZTONAL POSITIONING PERFORMANCES

	Robust EKF+C/N0 Thresholding	AREKF Tikhonov	AREKF with Optimal Reg. Matrix
Mean HPE [m]	9.25	8.86	7.5
Max HPE [m]	25.8	22.04	18.34
Mean BEE [m]	-	3.2	4.07
Max BEE [m]	-	34.25	37.02

V. CONCLUSIONS

Reliable GNSS positioning is difficult to be achieved in dense urban areas which slow down the adoption of GNSS in applications which require high service availability and good level of confidence in the position estimation. In this regard, efficient and timely solutions for the MP/NLOS problem are very much sought after. This research sheds new lights on a new sub-optimal regularization estimation of the user position and the PR bias for positioning performance enhancement.

In this work, we adopt the strategy of using constructively degraded measurement since excluding them may deteriorate position availability or adversely affect the satellites geometry. We propose to jointly estimate the position and the PR bias for PR measurements correction in harsh environments with mixed NLOS and MP receptions. Since this problem is overparameterized and the corresponding observation matrix has a large condition number, we have chosen to originally found a solution in the framework of regularization estimation. If well-tuned, regularization techniques give well-behaved estimator in overparameterized estimation problems. The main contribution of this work was the derivation of the optimal regularization parameters for efficiency maximization, in the sense of the total MSE. The found optimal parameter is verifying the best tradeoff between the variance and the bias of the estimation. This formulation has been validated using real GNSS measurements in an urban environment in Toulouse.

ACKNOWLEDGMENT

The authors would like to thank the French Space Agency (CNES) for funding this research project: SPRING Usage for Modeling Multipath Effects on a Receiver (SUMMER).

APPENDIX A

Using the following form of the diagonal matrix $\mathbf{T}_1 = \left(\mathbf{H}_0^T\mathbf{H}_0\right)^{-1}\mathbf{H}_0^T\mathbf{T}_2\mathbf{H}_0$ we have the following relation:

$$\mathbf{H}_0\mathbf{T}_1 = \mathbf{T}_2\mathbf{H}_0$$

By applying the transpose the last expression, we have also:

$$\mathbf{T}_1\mathbf{H}_0^T = \mathbf{H}_0^T\mathbf{T}_2$$

These two relations imply the following:

$$\mathbf{TA}_0 = \mathbf{A}_0\mathbf{T}; \quad \mathbf{TA}_T = \mathbf{A}_T\mathbf{T}; \quad \mathbf{A}_T^{-1}\mathbf{A}_0 = \mathbf{A}_0\mathbf{A}_T^{-1}$$

The OMSE expression is given by (10):

$$OMSE[\hat{\mathbf{x}}_T] = tr\left\{\mathbf{A}_T^{-2}\mathbf{TC}_{\mathbf{x}_1}\mathbf{T}\right\} + tr\left\{\sigma_v^2\mathbf{A}_T^{-2}\mathbf{A}_0\right\}$$

We start by differentiating the first term of the OMSE. We simplify it using the relations $\mathbf{TA}_0 = \mathbf{A}_0\mathbf{T}$ and $\mathbf{TA}_T = \mathbf{A}_T\mathbf{T}$:

$$tr\left\{\mathbf{A}_T^{-2}\mathbf{TC}_{\mathbf{x}_1}\mathbf{T}\right\} = tr\left\{\mathbf{C}_{\mathbf{x}_1}\right\} - 2tr\left\{\mathbf{C}_{\mathbf{x}_1}\mathbf{A}_0\mathbf{A}_T^{-1}\right\} + tr\left\{\mathbf{A}_0\mathbf{A}_T^{-1}\mathbf{C}_{\mathbf{x}_1}\mathbf{A}_T^{-1}\mathbf{A}_0\right\}$$

Differentiating the last expression over $\mathbf{A}_T^{-1}$ yields:

$$\frac{\partial tr\left\{\mathbf{A}_T^{-2}\mathbf{TC}_{\mathbf{x}_1}\mathbf{T}\right\}}{\partial \mathbf{A}_T^{-1}} = -2\mathbf{C}_{\mathbf{x}_1}\mathbf{A}_0 + 2\mathbf{C}_{\mathbf{x}_1}\mathbf{A}_0\mathbf{A}_T^{-1}\mathbf{A}_0 = -2\mathbf{C}_{\mathbf{x}_1}\mathbf{TA}_0\mathbf{A}_T^{-1}$$

The derivation of the second term of the OMSE expression over $\mathbf{A}_T^{-1}$ gives the following:

$$\frac{\partial tr\left\{\sigma_v^2\mathbf{A}_T^{-2}\mathbf{A}_0\right\}}{\partial \mathbf{A}_T^{-1}} = 2\sigma_v^2\mathbf{A}_0\mathbf{A}_T^{-1}$$

We obtain then the derivation of the OMSE over $\mathbf{A}_T^{-1}$:

$$\frac{\partial}{\partial \mathbf{A}_T^{-1}} OMSE[\hat{\mathbf{x}}_T] = 2\left(\sigma_v^2\mathbf{I} - \mathbf{C}_{\mathbf{x}_1}\mathbf{T}\right)\mathbf{A}_0\mathbf{A}_T^{-1}$$

By nothing that: $\frac{\partial \mathbf{A}_T^{-1}}{\partial \mathbf{T}} = -\mathbf{A}_T^{-2}$, expression (12) is proven.

APPENDIX B

We start from the expression of the minimal OMSE in (17):

$$OMSE[\hat{\mathbf{x}}_T]_{Min} = \sigma_v^2\begin{pmatrix} tr\left\{(\mathbf{I}_N + \mathbf{T}_2)^{-1}\right\} + \\ tr\left\{\left(\mathbf{I}_M + \mathbf{H}_0^T(\mathbf{I}_N + \mathbf{T}_2)^{-2}\mathbf{H}_0\right)\mathbf{M}_0\right\}\end{pmatrix}$$

In the case of Tikhonov regularization, i.e. $\mathbf{T}_2 = \gamma_{opt}\mathbf{I}_N$ and $\mathbf{T}_1 = \gamma_{opt}\mathbf{I}_M$, we have:

$$tr\left\{(\mathbf{I}_N + \mathbf{T}_2)^{-1}\right\} = \frac{N}{\gamma_{opt} + 1}$$

$$\begin{aligned}\mathbf{M}_0 &= \left(\mathbf{H}_0^T\mathbf{H}_0 + \mathbf{T}_1 - \mathbf{H}_0^T(\mathbf{I}_N + \mathbf{T}_2)^{-1}\mathbf{H}_0\right)^{-1} \\ &= \frac{(\gamma_{opt} + 1)}{\gamma_{opt}}\left(\mathbf{H}_0^T\mathbf{H}_0 + (\gamma_{opt} + 1)\mathbf{I}_M\right)^{-1}\end{aligned}$$

$$\left(\mathbf{I}_M + \mathbf{H}_0^T(\mathbf{I}_N + \mathbf{T}_2)^{-2}\mathbf{H}_0\right) = \frac{1}{(\gamma_{opt} + 1)^2}\left(\mathbf{H}_0^T\mathbf{H}_0 + (\gamma_{opt} + 1)^2\mathbf{I}_M\right)$$

By bringing together these three expressions, we get:

$$OMSE[\gamma_{opt}]_{Min} = \frac{\sigma_v^2}{\gamma_{opt}(\gamma_{opt} + 1)}\left(N\gamma_{opt} + tr\{\mathbf{J}\}\right)$$

Where $\mathbf{J} = \left(\mathbf{H}_0^T\mathbf{H}_0 + (\gamma_{opt} + 1)^2\mathbf{I}_M\right)\left(\mathbf{H}_0^T\mathbf{H}_0 + (\gamma_{opt} + 1)\mathbf{I}_M\right)^{-1}$

By nothing that: $(\gamma_{opt} + 1)^2\mathbf{I}_M = (\gamma_{opt} + 1)\mathbf{I}_M + \gamma_{opt}(\gamma_{opt} + 1)\mathbf{I}_M$

We can simplify **J** to:

$$\mathbf{J} = \mathbf{I}_M + \gamma_{opt}(\gamma_{opt} + 1)\left(\mathbf{H}_0^T\mathbf{H}_0 + (\gamma_{opt} + 1)\mathbf{I}_M\right)^{-1}$$

By linearity of the operator trace, we finally get:

$$tr\{\mathbf{J}\} = M + \gamma_{opt}(\gamma_{opt} + 1)\,tr\left\{\left(\mathbf{H}_0^T\mathbf{H}_0 + (\gamma_{opt} + 1)\mathbf{I}_M\right)^{-1}\right\}$$

This proves relation (18).

REFERENCES

[1] P. D. Groves, *Principles of GNSS, Inertial, and Multisensor Integrated Navigation Systems*. Artech House Publishers, 2nd Revised edition (1 mars 2013).

[2] S. Peyraud et al., "About Non-Line-Of-Sight Satellite Detection and Exclusion in a 3D Map-Aided Localization Algorithm," Sensors 2013.

[3] J. Marais, S. Tay, A. Flancquart, C. Meurie, "Weighting with the pre-knowledge of GNSS signal state of reception in urban areas,"ENC 2015.

[4] A. Bourdeau, M. Sahmoudi, J.-Y. Tourneret, "Tight Integration of GNSS and a 3D City Model for Robust Positioning in Urban Canyons," Proceedings of ION GNSS 2012, Nashville, TN, September 2012.

[5] K. A. Bin Ahmad, M. Sahmoudi, C. Macabiau, A. Bourdeau, G. Moura, "Reliable GNSS Positioning in Mixed LOS/NLOS Environments Using a 3D Model," European Navigation Conference 2014, Vienne, Austria.

[6] N. Kbayer, M. Sahmoudi, E. Chaumette, "Robust GNSS Navigation in Urban Environments by Bounding NLOS Bias of GNSS Pseudoranges Using a 3D City Model," Proceedings of ION GNSS+ 2015.

[7] A. J. Van Dierendonck, P. Fenton, T. Ford, "THEORY AND PERFORMANCE OF NARROW CORRELATOR SPACING IN A GPS RECEIVER," Journal of The Institute of Navigation, Vol. 39, No. 3, Fall 1992, pp. 265-284.

[8] M. Sahmoudi, R. Jr. Landry, "Multipath Mitigation Techniques Using Maximum-Likelihood Principles," Inside GNSS Magazine, November/December 2008. Invited Paper.

[9] I. Guvenc, C. C. Chong, "A Survey on TOA Based Wireless Localization and NLOS Mitigation Techniques," IEEE Communications Surveys & Tutorials, vol.11, no.3, pp.107-124, 3rd Quarter 2009.

[10] N. Kbayer, M. Sahmoudi, E. Chaumette, T. Chapuis, "Robust Kalman Filtering for NLOS Mitigation of GNSS Measurements in Urban Environments," European Navigation Conference (ENC 2015).

[11] A. Rabaoui, N. Viandier, J. Marais, E. Duflos, "Using Dirichlet Process Mixtures for the Modelling of GNSS Pseudorange Errors in Urban Canyon," Proceedings ION GNSS 2009, Savannah, GA, Sep. 2009.

[12] Y. Ng, G. X. Gao, "Direct Position Estimation Utilizing Non-Line-of-Sight (NLOS) GPS Signals," Proceedings of ION GNSS+ 2016.

[13] T. Suzuki, N. Kubo, "Correcting GNSS Multipath Errors Using a 3D Surface Model and Particle Filter," Proceedings ION GNSS+ 2013.

[14] D. Betaille, F. Peyret, M. Ortiz, S. Miquel, L. Fontenay, "A New Modeling Based on Urban Trenches to Improve GNSS Positioning Quality of Service in Cities," Intelligent Transportation Systems Magazine, IEEE , vol.5, no.3, pp.59-70, Fall 2013.

[15] P. Misra, P. Enge, Global Positioning System : Signals, Measurements and Performance. Ganga-Jamuna Press, 2001.

[16] T. Iwase, N. Suzuki, Y. Watanabe, "Estimation and exclusion of multipath range error for robust positioning," GPS Solution 2013.

[17] T. Ballal, T. Y. Al-Naffouri, (2015, April). Improved linear least squares estimation using bounded data uncertainty. In *IEEE International Conference on Acoustics, Speech and Signal Processing (ICASSP), 2015*. IEEE (pp. 3427-3431).

[18] D. P. Bertsekas, Nonlinear Programming, Second ed. Belmont, MA:Athena Scientific, 1999.

[19] M. Martinez-Camara, M. Muma, A. M. Zoubir, M. Vetterli, (2015, April). A new robust and efficient estimator for ill-conditioned linear inverse problems with outliers. In *IEEE International Conference on Acoustics, Speech and Signal Processing (ICASSP 2015).*

[20] J. Cai, C. Hu, E. W. Grafarend, (2007). The optimal regularization method and its application in GNSS Rapid Static Positioning. *ION GNSS Proceedings, Fort Worth*, 299-305.

[21] Q. Gui, K. Chen, Y. Gu, (2013). TSVD Regularization with Ill-Conditioning Diagnosis in GNSS Multipath Estimation. In *Proceedings of 2013 Chinese Intelligent Automation Conference* (pp. 421-429).

[22] A. N. Tikhonov, V. I. Arsenin, (1977). *Solutions of ill-posed problems* (Vol. 14). Washington, DC: Winston.